Dynamic Compressive Behavior of Thick Composite Materials

by H. M. Hsiao, I. M. Daniel and R. D. Cordes

ABSTRACT—The effect of strain rate on the compressive behavior of thick carbon/epoxy composite materials was investigated. Falling weight impact and split Hopkinson pressure bar systems were developed for dynamic characterization of composite materials in compression at strain rates up to 2000 s^{-1}. Strain rates below 10 s^{-1} were generated using a servohydraulic testing machine. Strain rates between 10 s^{-1} and 500 s^{-1} were generated using the drop tower apparatus. Strain rates above 500 s^{-1} were generated using the split Hopkinson pressure bar. Unidirectional carbon/epoxy laminates (IM6G/3501-6) loaded in the longitudinal and transverse directions, and $[(0_8/90_8)_2/\bar{0}_8]_s$ cross-ply laminates were characterized. The 90-deg properties, which are governed by the matrix, show an increase in modulus and strength over the static values but no significant change in ultimate strain. The 0-deg and cross-ply laminates show higher strength and ultimate strain values as the strain rate increases, whereas the modulus increases only slightly over the static value. The increase in strength and ultimate strain observed may be related to the shear behavior of the composite and the change in failure modes. In all cases, the dynamic stress-strain curves stiffen as the strain rate increases. The stiffening is lowest in the longitudinal direction and highest in the transverse direction.

KEY WORDS—Thick composites, strain rate effects, dynamic response, compressive testing of composites, falling weight impact, split Hopkinson pressure bar, compressive properties

Introduction

As composite materials become more attractive for large structures and hydrospace applications, understanding the compressive behavior of thick composite materials becomes necessary. The analysis and design of such structures subjected to dynamic loadings, ranging from low-velocity projectile impact to high-energy shock loadings, requires the input of high strain rate compressive properties. The effect of strain rate on material behavior cannot be neglected if reliable modeling approaches are to be made for simulations. Numerical simulations using finite element analysis require an accurate description of such effects as strain rate, loading history, load intensity, deformation and internal damage.

H. M. Hsiao (SEM Member) is Senior Materials Scientist, Hexcel Corporation, Dublin, CA 94568. I. M. Daniel (SEM Member) is Professor, Robert R. McCormick School of Engineering and Applied Science, Northwestern University, Evanston, IL 60208. R. D. Cordes (SEM Member) is with Vertech Systems, Inc., Houston, TX 77041.

Final manuscript received: January 24, 1998.

Most composite materials have been amply characterized under quasi-static conditions. Related work under dynamic conditions has been relatively limited due to the experimental difficulties of characterizing the high-rate behavior. Most of the dynamic work has involved lateral impact testing of composite laminates but has placed little emphasis on constitutive properties. To develop more sophisticated constitutive models and failure criteria under dynamic loading, experiments performed over a wide range of strain rates, in which a single dominant stress component can be isolated, are very important.

The first attempts to characterize composite materials under dynamic loading were carried out by Rotem and Lifshitz[1,2] and Sierakowski *et al.*[3] Most of the high strain rate compressive properties reported to date have been obtained by means of the split Hopkinson pressure bar technique.[3–8] Sierakowski *et al.* investigated steel/epoxy composites in compression up to 1000 s^{-1}. They observed very different failure modes in static and dynamic compressive tests on cylindrical specimens. The initial modulus remains unchanged, but the strength increases by 100 percent in the dynamic tests. Harding[5] studied two woven glass/epoxy material systems in compression up to 860 s^{-1} using cylindrical and thin strip specimens. He concluded that there is a significant increase in the initial modulus, strength and ultimate strain with increasing strain rate for woven glass/epoxy composites. Amijima and Fujii[9] studied glass/polyester plain woven and unidirectional composites in compressive tests of cylindrical specimens. The increase in strength is shown to be higher for the woven composites than for the unidirectional ones. Daniel and LaBedz[10] developed a test method using a thin graphite/epoxy (six to eight plies thick) composite ring specimen loaded by an external pressure pulse applied explosively through a liquid. They obtained compressive properties at strain rates up to 500 s^{-1}. The 0-deg properties show some increase in initial modulus over the static values but no change in strength. The 90-deg properties show much higher than static modulus and strength. Montiel and Williams[11] used an instrumented drop tower to determine compressive properties of 48-ply graphite/PEEK $[0_2/90]_{8s}$ composites for strain rates up to 8 s^{-1}. The results indicate that at high strain rate loading, the strength increases by 42 percent over static values, whereas the ultimate strain increases by 25 percent. There only appears to be a small strain rate effect on the initial modulus. Groves *et al.*[12] also developed a drop tower system to generate strain rates from 10 to 1000 s^{-1}. Review articles on high strain rate studies for composites were written by Greszczuk and Sierakowski.[13–15]

The various test methods used to date have different advantages and limitations. The use of a servohydraulic machine is common and convenient. It can produce excellent results without the noise problem. However, the method is limited to lower strain rates, below $10\ s^{-1}$, because of inertial effects of the load cell and grips. The drop weight impact test has many advantages: it is inexpensive, can accommodate different specimen geometries and allows easy variation of strain rate. However, the system is very sensitive to the contact conditions between the impactor and specimen and to spurious noise from ringing and vibrations. The induced stress waves are superimposed on the stress-strain curves measured and create difficulties in interpreting the experimental results. The split Hopkinson pressure bar technique permits testing at higher strain rates exceeding $1000\ s^{-1}$. Contact surface conditions are very critical. Specimens must be short to minimize wave propagation effects. However, this raises questions about the homogeneity and uniaxiality of the induced stress in the specimen, and thus a complex study of wave propagation effects in composite materials is required. The use of thin ring specimens under dynamic internal or external pressure minimizes the wave propagation effects, but it is expensive and complex and cannot be used for thick composites.

This paper discusses the application of a drop weight method and a split Hopkinson pressure bar technique for dynamic characterization of thick carbon/epoxy composites. Test methodology for high strain rate compressive testing of end-loaded thick composite specimens was developed. The results presented cover strain rates from quasi-static to $1800\ s^{-1}$.

Experimental Procedure

Material Selection and Specimen Fabrication

To investigate the strain rate effects in this study, 72- and 48-ply unidirectional laminates were selected. The material used was IM6G/3501-6 carbon/epoxy composite (Hexcel Corp.). The prepreg layup was cured in a press/autoclave by a three-step curing cycle especially developed for thick composites.[16]

Drop Tower Apparatus

A drop tower was designed and built for dynamic compressive testing of thick composites at strain rates ranging from 10 to several hundred per second.[17] The drop weight is guided along two 3-m (10-ft) long guide rods through bearing assemblies. It is raised and released using an electromagnet. A 5000-g quartz accelerometer (Kistler Instrument Corporation) is mounted at the center of the drop weight on the top surface.

Figure 1(a) shows the dynamic compression test specimen configuration for the drop tower. A 72-ply composite specimen 2.54 cm (1 in.) long and 1.27 cm (0.50 in.) wide was bonded to a similar high-strength steel specimen. The latter was made of 4140 steel with a yield stress of 1660 MPa (240 ksi) under quasi-static loading. Steel end caps were bonded at the outer ends. In all cases, the specimens were end loaded. A fixture was designed to hold and guide the specimen during impact [Fig. 1(b)]. Uniform end loading was accomplished through the use of this guide system to constrain all but the vertical motion of the specimen. The specimen with the end caps was mounted in such a way that the top of the end caps protruded by 6 mm (0.25 in.) above the top of the guide system. Axial strain gages were mounted on both sides of the composite and steel specimens, connected to a bridge conditioner, amplified by an HP amplifier and recorded by a digital-processing oscilloscope (Norland 3001) at sampling intervals of 1-10 μs. For strain rates below $10\ s^{-1}$, the servohydraulic testing machine was used, along with the specimen, guide fixture and data acquisition system described here.

The dynamic impact force was measured in two different ways. Initially, it was measured with an accelerometer mounted on the top of the drop weight. The dynamic force and hence applied stress was obtained from the accelerometer reading multiplied by the mass of the impactor assembly, which included the drop weight, bearing assembly and top end cap. This was checked against the value obtained more directly from strain readings on the steel portion of the specimen. The axial strain in the steel specimen (load cell), mounted in series with the composite specimen, was multiplied by its modulus (207 GPa; 30 Msi) for more accurate determination of the dynamic force. Typical results of a 72-ply unidirectional composite specimen under dynamic transverse compression are shown in Fig. 2, where dynamic transverse stress-strain curves are plotted based on both acceleration and steel calibration strain measurements. The force results obtained from the accelerometer reading were in agreement with those obtained from strain readings in the steel specimen. Discrepancies occurred near the end of the stress-strain curve, with the accelerometer reading giving a lower force value. This was attributed to wave propagation effects inside the impactor and vibrations of the entire system. Because of the noise from the accelerometer, force determinations based on steel strain readings were judged to be more reliable and were used in all cases.

The major problem in the use of a drop tower apparatus is the presence of vibration stress waves superimposed on the stress-strain curves. In this study, rubber sheets, from 2.54 mm (0.1 in.) to 7.62 mm (0.3 in.) thick, were placed over the top end cap to minimize ringing due to impact. Fiber cork vibration damping pads were placed between the floor and the entire drop tower apparatus to attenuate the transmitted waves. This acoustically damped base system reduced the spurious noise in the acceleration and strain readings caused by apparatus vibrations and steel-to-steel contact. It is noted that, without damping the system, the acceleration, load and strain measurements are distorted through oscillations, which include rigid body accelerations of the system and shock waves resulting from impact. The lower frequency data are attributable to rigid body acceleration, whereas the higher frequency data result from acoustic waves. To separate these two sources, a fast Fourier transform analysis can be applied to decompose the frequency of the raw data and to find a corrected signal corresponding to the real mechanical response of the material.[18,19]

Split Hopkinson Pressure Bar Apparatus

A split Hopkinson pressure bar was designed and built for dynamic compressive testing of composites for strain rates above several hundred per second.[17] It consists of a pneumatic loading device (pressure chamber, gun barrel and release valve), 7.6-cm (3-in.) to 15.2-cm (6-in.) long striker bars and two 1.27-cm (0.50-in.) diameter and 0.91-m (3-ft) long pressure-measuring bars. The bars in the split Hopkin-

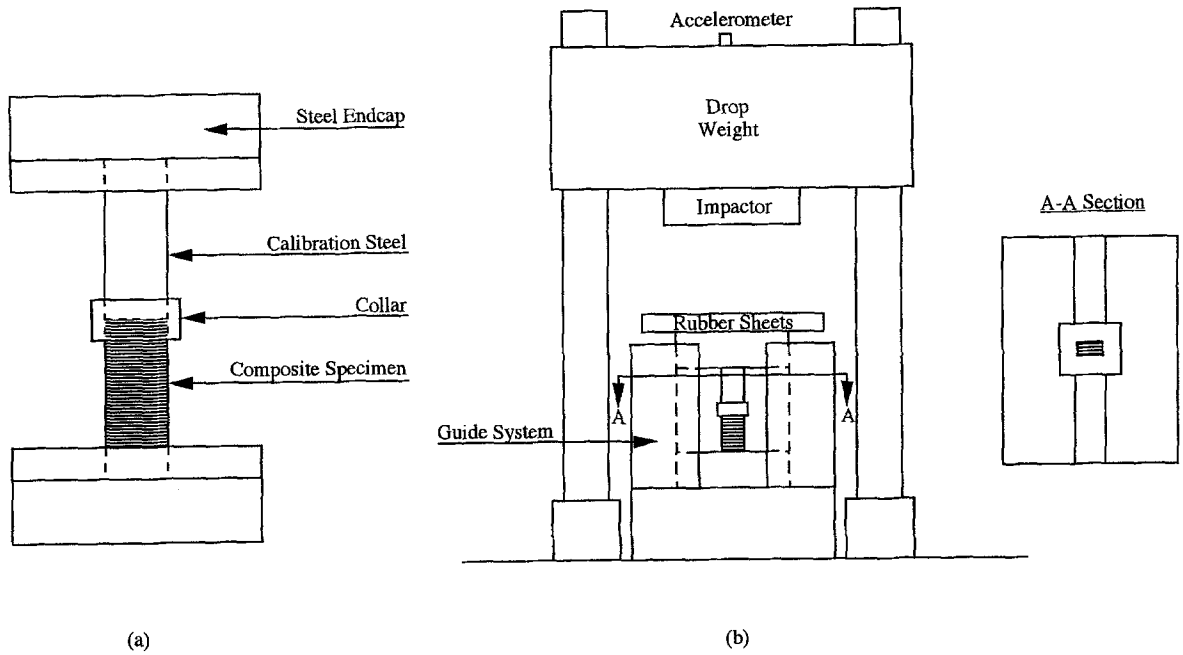

Fig. 1—(a) Impact specimen configuration, (b) specimen holding and guide fixture

son pressure bar system were made of 17-4 PH stainless steel with a yield strength of approximately 1240 MPa (180 ksi) under quasi-static loading. Short, rectangular 48-ply composite specimens, 9.53 mm (0.375 in.) long and 6.4 mm (0.25 in.) wide, were sandwiched between the two pressure bars. An air gun with a 1.21-m (4-ft) long gun barrel was used to propel the striker bar, which impacted directly on the free end of the input bar. Strain gages were mounted at the midpoint of the input and output bars and on the specimen itself to monitor the stress waves. The strain gages in this case were recorded at 100- to 400-ns intervals. The loads and displacements at both ends of the specimen were determined by monitoring the waves in the bars. A small rubber sheet was placed at the striker bar-incident bar interface to act as a wave shaper. This increases the pulse rise time during elastic loading of the specimen and increases the uniformity of loading in the specimen.

The split Hopkinson pressure bar technique has been used extensively for several decades. The equations for the analysis are based on one-dimensional wave theory in an infinite cylindrical solid and are widely reported in a number of references.[20,21] When the specimen deforms uniformly, the strain in the specimen is given by

$$\frac{d\varepsilon(t)}{dt} = \frac{C_0}{L}[\varepsilon_I(t) - \varepsilon_R(t) - \varepsilon_T(t)] \quad \text{or}$$
$$\frac{d\varepsilon(t)}{dt} = -\frac{2C_0}{L}\varepsilon_R(t) \tag{1}$$

and the stress by

$$\sigma(t) = \frac{E}{2}\frac{A_0}{A}[\varepsilon_I(t) + \varepsilon_R(t) + \varepsilon_T(t)] \quad \text{or}$$
$$\sigma(t) = E\frac{A_0}{A}\varepsilon_T(t), \tag{2}$$

since

$$\varepsilon_I(t) + \varepsilon_R(t) = \varepsilon_T(t), \tag{3}$$

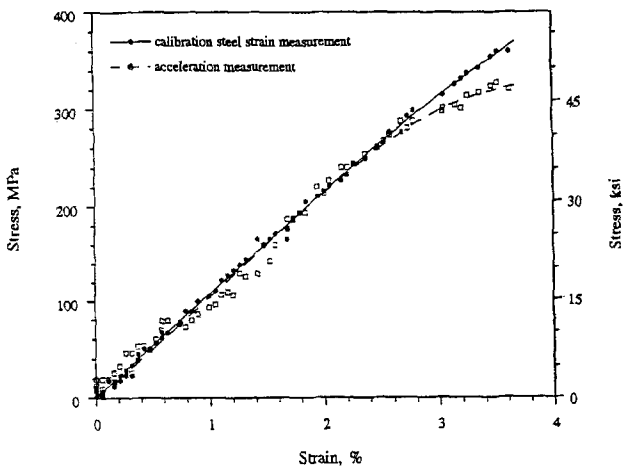

Fig. 2—Transverse compressive stress-strain curves for unidirectional IM6G/3501-6 carbon/epoxy at a strain rate of 60 s^{-1} (the curves are based on both acceleration and steel calibration strain measurements)

where C_0 is the longitudinal wave speed in the pressure bar; $\varepsilon_I(t)$, $\varepsilon_R(t)$, $\varepsilon_T(t)$ are the incident, reflected and transmitted strain pulses, respectively, measured from strain gages; L is the specimen length; E is Young's modulus of the pressure bar; and A_0, A is a cross-sectional area of the pressure bar and specimen, respectively.

The above expressions indicate that the dynamic stress-strain behavior of the specimen can be determined simply by strain measurements made on the surface of the pressure bars. However, it should be noted that the above equations require three important conditions to be met. The first condition is that wave propagation within the pressure bars be one dimensional, the second condition is that the specimen deform uniformly, and the third condition is that the pressure bars behave elastically. These conditions and limitations of

the split Hopkinson pressure bar experiment have been discussed extensively in a number of references.[22,23]

Results and Discussion

Transverse Compressive Behavior of Unidirectional Composite

High strain rate tests were performed on the drop tower and the split Hopkinson pressure bar. Tests conducted on the drop tower used a mass of 4.66 kg (10.27 lb) falling from a height of 2.44 m (8 ft), producing strain rates from 10 to several hundred per second. Tests conducted on the split Hopkinson pressure bar used air pressure from 276 kPa (40 psi) to 620 kPa (90 psi) to propel the striker bar. Variations in the striker bar length and kinetic energy resulted in specimen strain rates between several hundred and 2000 per second. Typical strain gage signals measured from the input and output bars are shown in Fig. 3.

The specimen strain is calculated from these strains by eq (1) and independently measured directly on the specimen. Typical specimen strain versus time curves are shown in Fig. 4. Because of the absorbers used, the initial portion of the strain-time curve was not truly indicative of the effective strain rate experienced by the specimen. However, the strain rate seemed to reach a nearly constant value at a strain level of approximately 10-20 percent of the ultimate strain. This is the strain rate referred to in the subsequent stress-strain curves.

Transverse stress-strain curves to failure under quasi-static and high strain rates are shown in Fig. 5. Table 1 summarizes the measured transverse compressive properties. This comparison shows a significant strain rate effect. The transverse strength, which is a matrix-dominated property, shows a nearly twofold increase from the quasi-static value. The initial modulus follows a similar trend, although not as pronounced, with an increase of up to 37 percent. The ultimate strain shows no strain rate effect at all, which implies that it can be used as a failure criterion in analysis under dynamic loading. Figure 5 also shows that the stress-strain behavior is a function of strain rate. The material stiffens (with

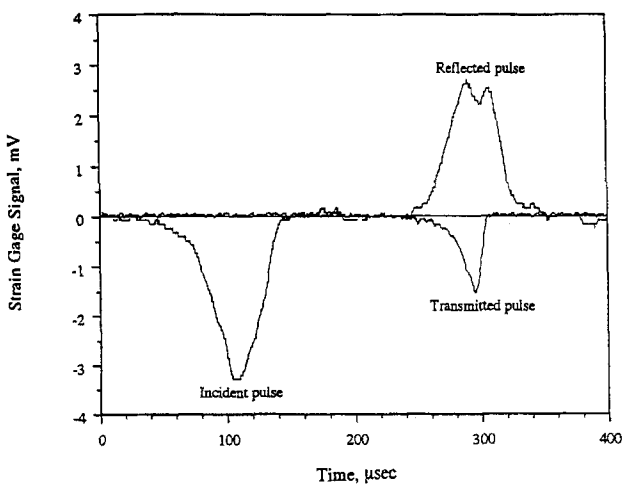

Fig. 3—The recorded stress wave profiles in the split Hopkinson pressure bar test for unidirectional IM6G/3501-6 carbon/epoxy under transverse compression

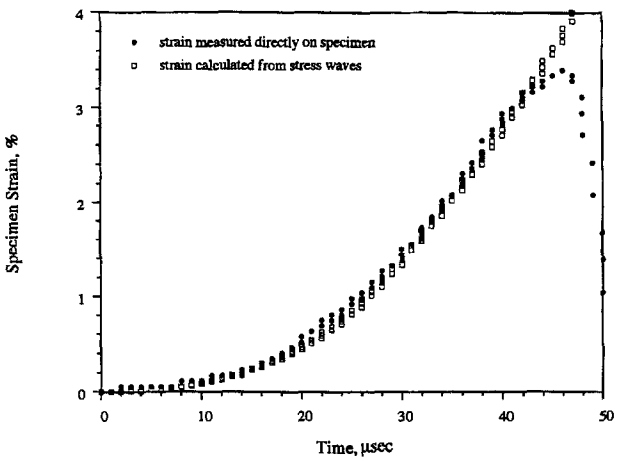

Fig. 4—Typical specimen strain versus time for a transversely loaded specimen in the split Hopkinson pressure bar apparatus

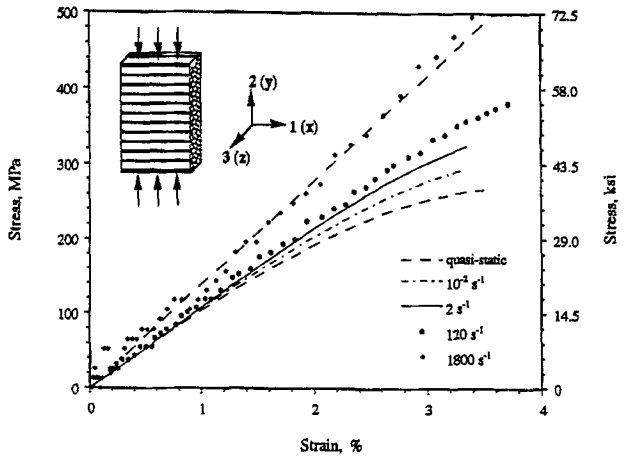

Fig. 5—Transverse compressive stress-strain curves for unidirectional IM6G/3501-6 carbon/epoxy under quasi-static and high strain rate loading

a reduction in matrix ductility) as the strain rate increases. This stiffening behavior is very significant in the nonlinear region between strain rates of 10^{-4} s^{-1} (quasi-static) and 1 s^{-1}. Above the strain rate of 1 s^{-1}, the stress-strain behavior continues stiffening until it is almost linear at a strain rate of 1800 s^{-1}. Two possible reasons for this phenomenon are proposed. The first is the viscoelastic nature of the polymeric matrix itself, and the second is the time dependent nature of accumulating damage. Evolution of damage is a time dependent phenomenon, and this in turn affects the time dependent (strain rate dependent) properties of the composite material.[24] At slower rates, damage accumulates more gradually such that a well-defined nonlinear region occurs near the end of the stress-strain curve. At higher rates, however, damage does not have enough time to develop, and thus the damage accumulation process has a diminishing effect on the stress-strain curve as the strain rate increases. More rigorous studies are needed before any definite conclusions can be reached.

Figure 6 shows the variation of the initial modulus and strength with strain rate. As shown in Fig. 6, two regions can be distinguished according to strain rate, which implies that the deformation mechanisms of the polymeric compos-

TABLE 1—TRANSVERSE COMPRESSIVE PROPERTIES OF UNIDIRECTIONAL IM6G/3501-6 CARBON/EPOXY COMPOSITE AT VARIOUS STRAIN RATES

Property Strain Rate	Modulus E_2, GPa (Msi)	Percentage Change	Strength F_{2c} MPa (ksi)	Percentage Change	Ultimate Strain ε_{2c}^{u} %	Percentage Change
$10^{-4}s^{-1}$	10.0 GPa (1.45 Msi)	—	269 MPa (39 ksi)	—	3.49	—
$10^{-2}s^{-1}$	10.7 GPa (1.55 Msi)	+7%	295 MPa (43 ksi)	+10%	3.34	−4%
$2\ s^{-1}$	10.8 GPa (1.56 Msi)	+8%	324 MPa (47 ksi)	+21%	3.35	−4%
$60\ s^{-1}$	11.0 GPa (1.59 Msi)	+10%	372 MPa (54 ksi)	+39%	3.69	+6%
$120\ s^{-1}$	11.4 GPa (1.66 Msi)	+15%	386 MPa (56 ksi)	+44%	3.74	+7%
$200\ s^{-1}$	11.0 GPa (1.60 Msi)	+10%	386 MPa (56 ksi)	+44%	3.75	+7%
$250\ s^{-1}$	12.5 GPa (1.81 Msi)	+25%	379 MPa (55 ksi)	+41%	3.65	+5%
$1500\ s^{-1}$	13.6 GPa (1.97 Msi)	+36%	459 MPa (67 ksi)	+71%	3.40	−3%
$1800\ s^{-1}$	13.7 GPa (1.99 Msi)	+37%	522 MPa (76 ksi)	+94%	3.64	+4%

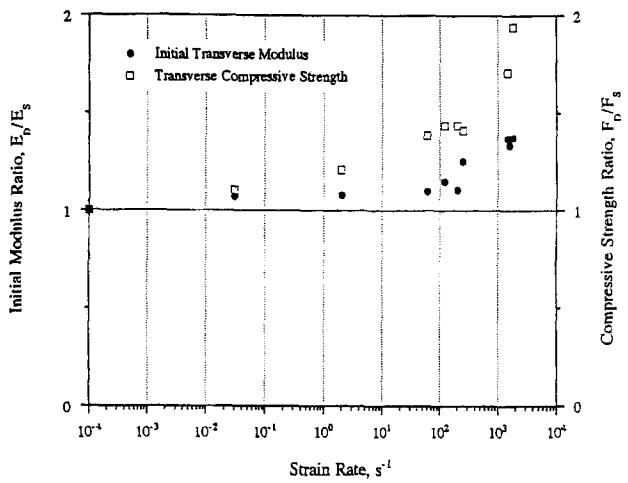

Fig. 6—Variation of initial transverse modulus and transverse compressive strength with strain rate

ite could change as the strain rate increases. In the first region, corresponding to strain rates between quasi-static and approximately 10 s^{-1}, there is a linear dependence of strength/modulus on the logarithm of strain rate. In the second region, corresponding to higher strain rates (above 10 s^{-1}), the strength/modulus seems to be a power function or exponential-like function of strain rate. Polymer viscoelasticity suggests that shear flow is highly impeded at high strain rates, and correspondingly the relaxation modulus has an exponential-like increase for very short loading durations.[12,25] Williams[26] observed that the fracture toughness of some polymers increases exponentially with strain rate. A reason for the increase in fracture toughness could be related to the restricted shear flow in the polymer. This would restrict the deformation of the polymer, which could in turn decrease the crack growth rate.

Longitudinal Compressive Behavior of Unidirectional Composite

Unidirectional specimens were loaded in the fiber direction with a mass of 17.31 kg (38.16 lb) falling from a height of 2.44 m (8 ft) in the drop tower. Typical steel and composite specimen strains versus time plots are shown in Fig. 7, from which the dynamic longitudinal stress-strain curve was obtained (Fig. 8). As in the case of transverse compression, an effective strain rate was defined as the nearly constant rate achieved above 20 percent of the ultimate strain. The strain rate attained in this case was approximately 110 s^{-1}.

In this study, the end-loading principle was adopted to test thick composites because it is widely accepted and, more important, easy to use for dynamic compressive testing. Test methods based on the end-loading principle include ASTM D695 test (SACMA SRM 1-88), European version

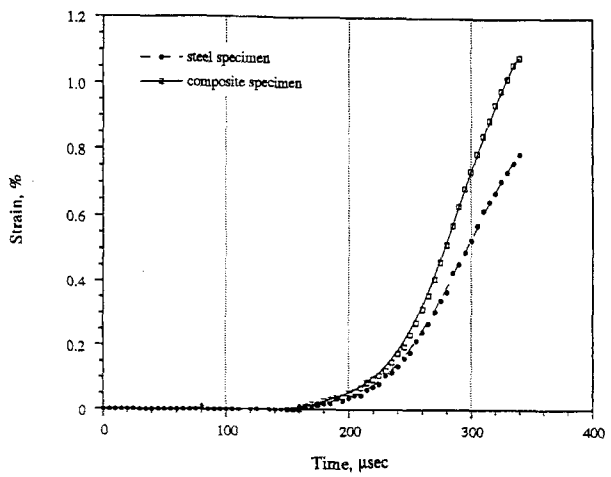

Fig. 7—Axial strains in longitudinally impacted unidirectional IM6G/3501-6 carbon/epoxy and calibration steel specimens (impactor mass = 17.31 kg [38.16 lb], height of drop = 2.44 m [8 ft])

ICSTM test[27] and DTRC test.[28] Recently, a new compression test method for thick composites (NU method) based on the concept of combined shear loading and end loading was developed.[29] It was found that the pure end-loading method tends to underestimate the longitudinal compressive strength and strain values due to premature end-crushing failure (Fig. 9). By using the NU test method, longitudinal compressive strengths of 1660 MPa (240 ksi), which are approximately 70 percent higher than those measured by the end-loading methods, are obtainable experimentally for thick composites under quasi-static loading. Therefore, experimental results from compression tests have to be interpreted with extra care. Longitudinal compressive strength and strain can only be compared when the same loading method is used.

Figure 10 displays the longitudinal stress-strain curves to failure under quasi-static and high strain rates of loading. It clearly shows the stiffening behavior in the nonlinear range that is not observable from the end-loading results alone. The stress-strain curve stiffens as the strain rate increases, although the magnitude of the change is much smaller compared to the transverse behavior. Table 2 summarizes the measured longitudinal compressive properties from the end-loading results alone. The initial modulus shows only a slight increase with strain rate. The strength and ultimate strain are significantly higher than the static values by up to 79 percent and 74 percent, respectively. Figure 11 shows the variation of the strength with strain rate. The increase in strength and ultimate strain observed may be related to the shear behavior of the composite and the change in failure modes. It is known that longitudinal compressive failure is intimately related to and governed by the in-plane shear response of the composite, even in the presence of the slightest initial fiber misalignment.[30–32] Any compressive failure observed follows some form of initial shear failure of the composite. The longitudinal compressive strength is expressed as[32]

$$F_{1c} = (\sigma_x)_{\max} = \frac{\tau^*}{\varphi + \gamma^*} \tag{4}$$

where φ is the initial fiber misalignment and τ^*, γ^* are values of shear stress and strain as defined in Fig. 12.

Figure 12 shows a measured shear stress-strain curve for IM6G/3501-6 carbon/epoxy composite with an illustration of a graphical determination of τ^* and γ^*. The compressive strength corresponds to the values τ^* and γ^*, where

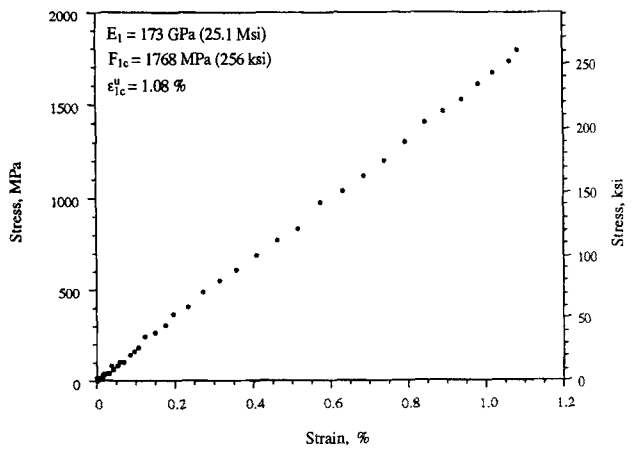

Fig. 8—Longitudinal compressive stress-strain curve for unidirectional IM6G/3501-6 carbon/epoxy at a strain rate of 110 s^{-1}

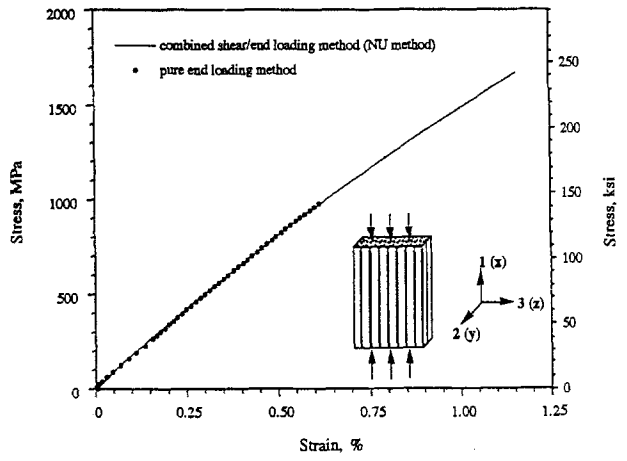

Fig. 9—Comparison of stress-strain curves between combined shear/end loading (NU test method) and pure end loading under quasi-static compressive loading

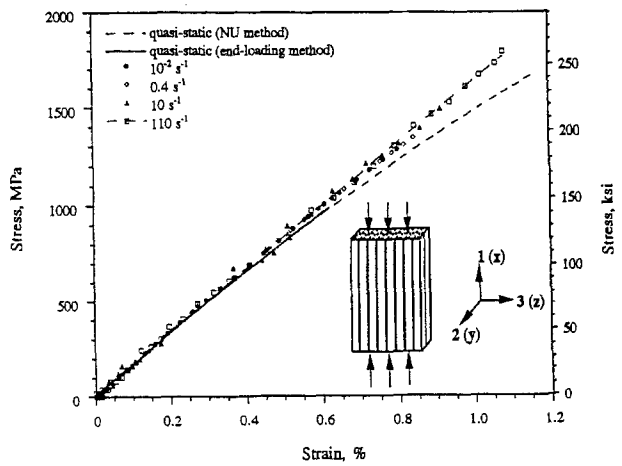

Fig. 10—Longitudinal compressive stress-strain curves for unidirectional IM6G/3501-6 carbon/epoxy under quasi-static and high strain rate loading

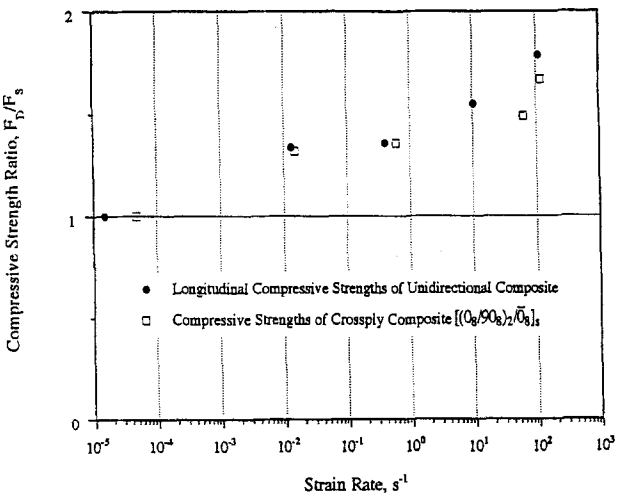

Fig. 11—Variation of compressive strength with strain rate for unidirectional and cross-ply IM6G/3501-6 carbon/epoxy

TABLE 2—LONGITUDINAL COMPRESSIVE PROPERTIES OF UNIDIRECTIONAL IM6G/3501-6 CARBON/EPOXY COMPOSITE AT VARIOUS STRAIN RATES

Property Strain Rate	Modulus E_1, GPa (Msi)	Percentage Change	Strength F_{1c} MPa (ksi)	Percentage Change	Ultimate Strain ε^u_{1c} %	Percentage Change
$10^{-5}s^{-1}$[a]	171 GPa (24.8 Msi)	—	1669 MPa (242 ksi)	—	1.16	—
$10^{-5}s^{-1}$	171 GPa (24.8 Msi)	—	987 MPa (143 ksi)	—	0.62	—
$10^{-2}s^{-1}$	172 GPa (25.0 Msi)	+0.6%	1316 MPa (191 ksi)	+34%	0.82	+32%
$0.4\ s^{-1}$	172 GPa (25.0 Msi)	+0.6%	1346 MPa (195 ksi)	+36%	0.84	+35%
$10\ s^{-1}$	173 GPa (25.1 Msi)	+1.2%	1530 MPa (222 ksi)	+55%	0.94	+52%
$110\ s^{-1}$	173 GPa (25.1 Msi)	+1.2%	1768 MPa (256 ksi)	+79%	1.08	+74%

a. Tests conducted by the combined shear/end loading method (NU method).

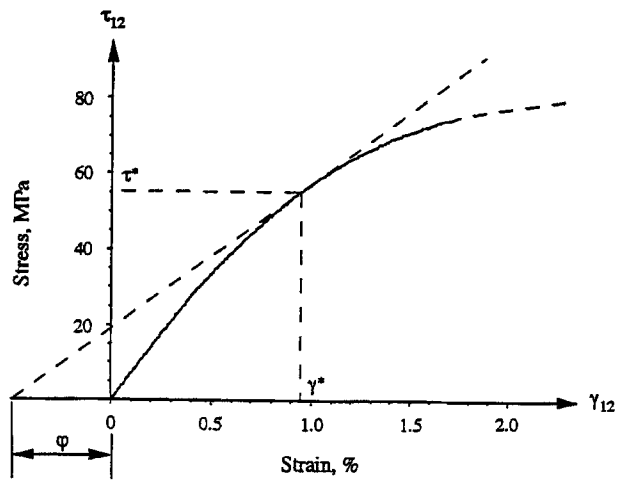

φ = initial fiber misalignment

Fig. 12—Graphical determination of longitudinal compressive strength

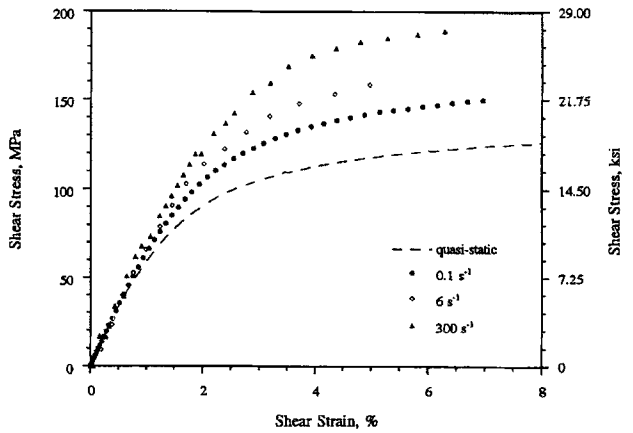

Fig. 13—Shear stress-strain curves from 45-deg off-axis unidirectional IM6G/3501-6 carbon/epoxy under quasi-static and high strain rate loading

the tangent to the shear stress-strain curve equals the slope $\tau^* = (\varphi + \gamma^*)$. It is apparent from Fig. 12 that if the in-plane shear behavior stiffens substantially with increasing strain rate, then this will lead to an increase in longitudinal compressive strength. Figure 13 shows the shear stress-strain curves obtained from 45-deg off-axis specimens under quasi-static and high strain rates. This comparison reveals a strong strain rate effect on the in-plane shear behavior of composites. The shear stress-strain behavior, which is matrix dominated, shows high nonlinearity with a plateau region at a stress level that increases significantly as the strain rate increases. Figures 12 and 13 offer a good explanation for the increase in longitudinal strength and ultimate strain observed. This relationship can also be used to explain the significant increase observed in the compressive strength of woven composites. It is found that a woven composite is more sensitive to strain rate than a unidirectional one, and that different woven composites have different strain rate effects due to the reinforcement structure.[9,33] Plain-weave composites show a higher strain rate effect than satin-weave, unidirectional or multidirectional composites. This is attributed to the higher shear dependence in the plain-weave case than in the other cases.

In addition, for high strain rate testing, the duration of loading is short enough that material failure occurs prior to the onset of fiber microbuckling. This suggests that a change in failure mode occurs as the strain rate increases. The microstructure change during high-rate testing should be studied in depth to elucidate the contribution of different damage mechanisms to the dynamic behavior of composite materials.

Compressive Properties of Cross-ply Composite

Cross-ply specimens of $[(0_8/90_8)_2/\bar{0}_8]_s$ layup were loaded with a mass of 11.34 kg (25 lb) falling from a height of 2.44 m (8 ft). Stress-strain curves to failure under quasi-static and high strain rate loading are shown in Fig. 14 for comparison. Figure 14 shows that the material stiffens as the strain rate increases and the magnitude of the change is slightly higher than in the longitudinal case. Table 3 summarizes the measured compressive properties. The initial modulus shows only a slight increase with strain rate. The strength and ulti-

TABLE 3—COMPRESSIVE PROPERTIES OF $[(0_8/90_8)_2/\bar{0}_8]_s$ CROSS-PLY IM6G/3501-6 CARBON/EPOXY COMPOSITE AT VARIOUS STRAIN RATES

Property Strain Rate	Modulus E_x, GPa (Msi)	Percentage Change	Strength F_{xc} MPa (ksi)	Percentage Change	Ultimate Strain ε^u_{xc}%	Percentage Change
$10^{-4}s^{-1}$[a]	96.5 GPa (14.0 Msi)	—	1131 MPa (164 ksi)	—	1.43	—
$10^{-4}s^{-1}$	98.6 GPa (14.3 Msi)	—	759 MPa (110 ksi)	—	0.83	—
$10^{-2}s^{-1}$	100 GPa (14.5 Msi)	+1.4%	1000 MPa (145 ksi)	+32%	1.12	+35%
$0.6\ s^{-1}$	100 GPa (14.5 Msi)	+1.4%	1035 MPa (150 ksi)	+36%	1.17	+41%
$60\ s^{-1}$	100 GPa (14.5 Msi)	+1.4%	1129 MPa (164 ksi)	+49%	1.21	+46%
$120\ s^{-1}$	102 GPa (14.8 Msi)	+3.5%	1266 MPa (184 ksi)	+67%	1.30	+57%

a. Tests conducted by the combined shear/end loading method (NU method).

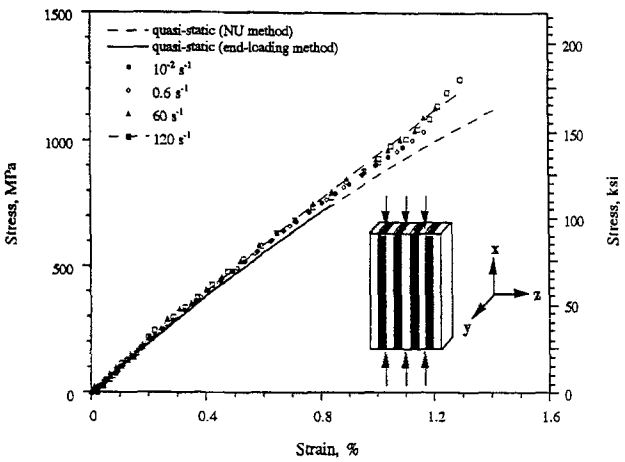

Fig. 14—Compressive stress-strain curves for $[(0_8/90_8)_2/\bar{0}_8]_s$ cross-ply IM6G/3501-6 carbon/epoxy under quasi-static and high strain rate loading

mate strain are significantly higher than the static values by up to 67 percent and 57 percent, respectively. Figure 11 shows the variation of the strength with strain rate. The strain rate sensitivity of the strength, initial modulus and ultimate strain of the cross-ply composite follow similar trends as those observed under longitudinal compression. Therefore, compressive behavior of a cross-ply composite is dominated by the 0-deg layers.

Summary and Conclusions

A systematic investigation was conducted on the effect of strain rate on the compressive behavior of thick composite materials. Unidirectional carbon/epoxy laminates (IM6G/3501-6) with fibers at 0 deg and 90 deg with the loading direction and $[(0_8/90_8)_2/\bar{0}_8]_s$ cross-ply laminates were characterized at strain rates up to 1800 s^{-1}.

The transverse compressive strength increases sharply with strain rate to nearly double the quasi-static value at the highest rate. The initial modulus follows a similar trend, although not as pronounced, with an increase of up to 37 percent. The ultimate strain shows no strain rate effect at all, which implies that it can be used as a failure criterion for analysis under dynamic loading. The stress-strain behavior is also a strong function of strain rate. The material stiffens significantly as the strain rate increases.

Longitudinal compressive properties were obtained for strain rates up to 110 s^{-1}. The initial modulus increases only slightly with strain rate over the static value. The strength and ultimate strain are significantly higher than the static values by up to 79 percent and 74 percent, respectively. The increase in strength and ultimate strain observed may be related to the stiffening of the composite in-plane shear behavior under dynamic loading and the change in failure modes. The stress-strain curve stiffens slightly as the strain rate increases. Compressive properties of a cross-ply composite were also obtained. The results show increases in strength and ultimate strain but only a slight increase in initial modulus. The stress-strain curve stiffens as the strain rate increases, and the magnitude of the change is slightly higher than in the longitudinal case. The strain rate sensitivities of the strength, initial modulus and ultimate strain of the cross-ply composite follow similar trends as those observed under longitudinal compression. Therefore, compressive behavior of cross-ply composite is dominated by the 0-deg layers.

Acknowledgments

The work described in this paper was sponsored by the Office of Naval Research (ONR). We are grateful to Dr. Y.D.S. Rajapakse of ONR for his encouragement and cooperation and to Mrs. Yolande Mallian for typing the manuscript.

References

1. Rotem, A. and Lifshitz, J.M., "Longitudinal Strength of Unidirectional Fibrous Composite Under High Rate of Loading," Proc. 26th Annual Tech. Conf. Soc. Plastics Industry, Reinforced Plastics/Composites Division, Washington, DC, Section 10-G, 1–10 (1971).

2. Lifshitz, J.M., "Impact Strength of Angle Ply Fiber Reinforced Materials," J. Composite Mat., **10** *(1), 92–101 (1976).*

3. Sierakowski, R.L., Nevil, G.E., Ross, A., and Jones, E.R., "Dynamic Compressive Strength and Failure of Steel Reinforced Epoxy Composites," J. Composite Mat., **5** *(3), 362–377 (1971).*

4. El-Habak, A.M.A., "Mechanical Behavior of Woven Glass Fibre-reinforced Composites Under Impact Compression Load," Composites, **22** *(2), 129–134 (1991).*

5. Harding, J., "Effect of Strain Rate and Specimen Geometry on the Compressive Strength of Woven Glass-reinforced Epoxy Laminates," Composites, **24** *(4), 323–332 (1993).*

6. Lifshitz, J.M. and Leber, H., "Data Processing in the Split Hopkinson Bar Tests," Int. J. Impact Eng., **15** (6), 723–733 (1994).

7. Powers, B.M., Vinson, J.R., Wardle, M., and Scott, B., "High Strain Rate Effects on AS4/PEEK Graphite Fiber Thermoplastic Matrix Composites," Proc. American Society for Composites, ed. W.S. Johnson, 486–494 (1996).

8. Weeks, C.A. and Sun, C.T., "Nonlinear Rate Dependent Response of Thick-section Composite Laminates," High Strain Rate Effects on Polymer, Metal and Ceramic Matrix Composites and Other Advanced Materials, ASME **AD-48**, ed. Y.D.S. Rajapakse and J.R. Vinson, 81–95 (1995).

9. Amijima, S. and Fujii, T., "Compressive Strength and Fracture Characteristics of Fiber Composites Under Impact Loading," Proc. 3rd Int. Conf. Composite Materials, ICCM III, ed. A.R. Russell, Paris, 399–413 (1980).

10. Daniel, I.M. and LaBedz, R.H., "Method for Compression Testing of Composite Materials at High Strain Rates," Compression Testing of Homogeneous Materials and Composites, ASTM STP 808, ed. R. Chait and R. Papirno, American Society for Testing and Materials, Philadelphia, PA, 121–139 (1983).

11. Montiel, D.M. and Williams, C.J., "A Method for Evaluating the High Strain Rate Compressive Properties of Composite Materials," Composite Materials: Testing and Design, ASTM STP 1120, ed. G.C. Grimes, American Society for Testing and Materials, Philadelphia, PA, **10**, 54–65 (1992).

12. Groves, S.E., Sanchez, R.J., Lyon, R.E., and Brown, A.E., "High Strain Rate Effects for Composite Materials," Composite Materials: Testing and Design, ASTM STP 1206, ed. E.T. Camponeschi, American Society for Testing and Materials, Philadelphia, PA, **11**, 162–176 (1993).

13. Greszczuk, L.B., "Damage in Composite Materials Due to Low Velocity Impact," Impact Dynamics, John Wiley & Sons, New York, Chap. 3 (1982).

14. Sierakowski, R.L., "High Strain Rate Testing of Composites," Proc. Dynamic Constitutive Failure Models, AFWAL-TR-88-4229, ed. A.M. Rajendran and T. Nicholas (December 1988).

15. Sierakowski, R.L., "Strain Rate Behavior of Composites: Issues," High Strain Rate Effects on Polymer, Metals and Ceramic Matrix Composites and Other Advanced Materials, ASME **AD-48**, ed. Y.D.S. Rajapakse and J.R. Vinson, 1–5 (1995).

16. Daniel, I.M., Hsiao, H.M., Wooh, S.C., and Vittoser, J., "Processing and Compressive Behavior of Thick Composites," Mechanics of Thick Composites, ASME **AMD-162**, ed. Y.D.S. Rajapakse, 107–126 (1993).

17. Hsiao, H.M., Daniel, I.M., and Cordes, R.D., "Strain Rate Effects on the Transverse Compressive and Shear Behavior of Unidirectional Composites," J. Composite Mat. (1996).

18. Tzeng, J.T. and Abrahamian, A.S., "Dynamic Compressive Properties of Laminated Composites at High Rates of Loading," Proc. American Society for Composites, ed. W.S. Johnson, 178–188 (1996).

19. Winkel, J.D. and Adams, D.F., "Instrumented Drop Weight Impact Testing of Crossply and Fabric Composites," Composites, **16** (4), 268–278 (1985).

20. Kolsky, H., "An Investigation of the Mechanical Properties of Materials at Very High Rates of Loading," Proc. Phys. Soc. Lon., Series B, **62**, 676–700 (1949).

21. Follansbee, P.S., "The Hopkinson Bar," Metals Handbook, **8**, 9th ed., 198–203 (1985).

22. Follansbee, P.S. and Frantz, C., "Wave Propagation in the Split Hopkinson Pressure Bar," Trans. ASME, J. Eng. Mat. Tech., **105** (1), 61–66 (1983).

23. Lataillade, J.-L., Bacon, C., Collombet, F., and Delaet, M., "The Benefit of Hopkinson Bar Techniques for the Investigation of Composite and Ceramic Materials," Wave Propagation and Emerging Technologies, ASME **AMD-188**, 85–94 (1994).

24. Raghavan, J. and Meshii, M., "Time-dependent Damage in Carbon Fibre-reinforced Polymer Composites," Composites Part A, **27A** (12), 1223–1227 (1996).

25. Christensen, R.M., Theory of Viscoelasticity, Academic Press, New York (1971).

26. Williams, J.G., Fracture Mechanics of Polymers, Ellis Horwood, London (1984).

27. Häberle, J.G. and Matthews, F.L., "An Improved Technique for Compression Testing of Unidirectional Fibre-reinforced Plastics: Development and Results," Composites, **25**, 358–371 (1994).

28. Camponeschi, E.T., Jr., "Compression Testing of Thick-section Composite Materials," Composite Materials: Fatigue and Fracture, ASTM STP 1110, American Society for Testing and Materials, Philadelphia, PA, 439–456 (1991).

29. Hsiao, H.M., Daniel, I.M., and Wooh, S.C., "A New Compression Test Method for Thick Composites," J. Composite Mat., **29** (13), 1789–1806 (1995).

30. Budiansky, B., "Micromechanics," Computer Struct., **16**, 3–12 (1983).

31. Häberle, J.G. and Matthews, F.L., "A Micromechanics Model for Compressive Failure of Unidirectional Fibre-reinforced Plastics," J. Composite Mat., **28** (17), 1618–1639 (1994).

32. Daniel, I.M., Hsiao, H.M., and Wooh, S.C., "Failure Mechanisms in Thick Composites Under Compressive Loading," Composites Part B, **27B** (6), 543–552 (1996).

33. Barre, S., Chotard, T., and Benzeggagh, M.L., "Comparative Study of Strain Rate Effects on Mechanical Properties of Glass Fibre-reinforced Thermoset Matrix Composites," Composites Part A, **27A** (12), 1169–1181 (1996).